ADVANCEMENT OF TECHNIQUES FOR MODELING THE EFFECTS OF FINE-SCALE ATMOSPHERIC INHOMOGENEITIES ON INFRASOUND PROPAGATION

Robert G. Gibson[1], Douglas P. Drob[2], and David Broutman[2]

BBN Technologies[1] and the Naval Research Laboratory[2]

Sponsored by the National Nuclear Security Administration

Award Nos. DE-AC52-08NA28652[1] and DE-AI52-08NA28653[2].
Proposal No. BAA08-05

ABSTRACT

Propagation studies of a growing number of infrasound observations indicate that fine-scale atmospheric inhomogeneities contribute to infrasonic arrivals that are not predicted by standard modeling techniques. In particular, gravity waves, or buoyancy waves, are believed to contribute to the multipath nature of infrasound propagation and to cause penetration of infrasound into the classical shadow zones that are predicted by conventional modeling techniques. Propagation modeling studies using simplified parameterizations of gravity wave spectra suggest that gravity waves represent the primary component of fine-scale atmospheric inhomogeneity that affects infrasonic arrivals at regional ranges.

The influence of atmospheric gravity waves on the upper atmosphere provides a significant source of geophysical uncertainty in atmospheric specifications. A large fraction of the gravity wave spectrum in operational numerical weather prediction models is either filtered out during the data assimilation process or else not resolved by the models. Existing approaches to modeling infrasound through gravity waves have relied on one-dimensional vertical wavenumber spectral models of gravity waves. This simplified model approach captures the vertical spatial scales in gravity waves as a function of height. Improved resolution of these wave fields through more sophisticated computational techniques to achieve more complete spectral parameterization is an important research challenge.

Atmospheric specification techniques are being developed that incorporate realistic models of gravity waves that are self-consistent with the background flow field and that include effects of altitude, range-dependence, and time-dependence over relevant scales. One shortcoming of existing gravity wave field models currently used with infrasound propagation models is that they ignore the typically strong refraction of the background gravity waves by variations in the mean winds and mean stratification above 15 km. These limitations are addressed by including the refraction effects of the gravity wave field by the background atmosphere as defined by the NRL-G2S semi-empirical specification. A local atmospheric gravity wave field is represented using the summation of vertical eigenfunctions approximated by a computationally efficient Fourier-space ray-tracing technique. Using this methodology, wave perturbation fields (horizontal wind components, pressure, density, and temperature) are calculated that are self-consistent with the background atmospheric flow.

Broadband, full-wave infrasound predictions computed using the parabolic equation (PE) method are used to model atmospheric infrasound from explosions at ranges of 100s to 1000s of km. Model predictions using the PE method are conducted using range-dependent specifications of the atmosphere from NRL-G2S that are modified by the addition of perturbation terms to the mean atmospheric wind profiles to represent gravity wave effects, in order to characterize the fine-scale atmospheric structure not resolved by numerical weather prediction models. Synthesized infrasound waveforms, obtained using the Fourier-synthesis time-domain PE method, are compared with observed infrasound signals from ground-truth events in order to evaluate the modeling capabilities.

OBJECTIVES

The objective of this research effort is to improve understanding of the effects of gravity waves and other fine-scale atmospheric inhomogeneities on infrasound propagation. The improved understanding of the relevant atmospheric and infrasonic physics will result in enhanced capabilities for modeling infrasound features and waveforms.

It is evident that existing propagation modeling, coupled with state-of-the-art atmospheric characterizations, fails to adequately predict infrasonic arrivals in all circumstances. In particular, there have been numerous events for which infrasound arrivals are observed by sensors in regions that are predicted by standard modeling techniques to be in shadow zones (e.g., Bhattacharyya et al., 2003; Kulichkov, 2004; Mutschlecner and Whitaker, 2006). This issue is relevant over both local and regional ranges. Recent scientific work in gravity waves, long-range acoustic propagation, and infrasound has indicated that fine-scale atmospheric inhomogeneities contribute to unexpected infrasonic arrivals. We endeavor to address this issue through systematic evaluation of the relevant atmospheric phenomena, advancement of the state of the art of modeling the interactions between fine-scale atmospheric inhomogeneities and infrasound, improved atmospheric specification, and model validation.

Specifically, the objectives are as follows:

- Review recent scientific progress in the understanding of gravity waves, their temporal and spatial variability, and their statistics, in order to develop an improved model of the characteristics of gravity waves that are relevant to infrasound propagation.
- Develop atmospheric specification techniques that incorporate realistic models of gravity waves in a manner that maintains self-consistency with the background flow field and that includes effects of latitude, longitude, and time-evolution over relevant scales.
- Exercise the improved gravity wave models with infrasound propagation models. Examine variability of infrasound predictions over a statistical ensemble of gravity wave realizations. Perform sensitivity studies to establish the effects of key atmospheric model variables on infrasound prediction.
- Perform model validation studies using ground truth datasets, focusing on local and regional ranges.

The effort is anticipated to increase understanding of the regional and local propagation of infrasound through the dynamic atmosphere and also to improve the capability to predict infrasound arrivals and features relevant to phase classification. Research results are anticipated to include spectral-based atmospheric variability specifications; numerical modeling subroutines that enable improved propagation modeling via incorporation of effects of gravity waves and related fine-scale atmospheric structure phenomena; and a summary of model/data comparison results.

RESEARCH ACCOMPLISHED

Atmospheric Specification

The atmospheric structure responsible for the propagation of infrasound can change rapidly. Global climatological models have largely been replaced in current infrasound modeling practice by the NRL Ground to Space (G2S) model of Drob et al. (2003) and Drob (2004), which was developed to provide background atmospheric information for the Nuclear Explosion Monitoring Research and Development program. The G2S data processing system combines operational numerical weather prediction (NWP) specifications with the upper atmospheric empirical models, NRLMSISE-00 and HWM-93 (Picone et al., 2002; Hedin et al., 1996). The near-real-time system incorporates 1ºx1º and 1ºx1.25º resolution global NWP input fields to the nearest 6-hour interval in the lower atmosphere. The HWM-93 model was recently upgraded to HWM-07 by Drob et al. (2008) via the assimilation of recent upper atmospheric research satellite-based measurements and ground-based measurements.

However, these specifications are unable to resolve all fine-scale stochastic phenomena, e.g., atmospheric irregularities smaller than the model resolution, fine-scale structures above 35 km, and gravity wave fluctuations that cannot be deterministically measured or internally generated by the model. Fine-scale atmospheric structure not characterized by near-real-time atmospheric models such as G2S has been identified as a likely source of refraction, advection and scattering effects that may play a significant role in infrasound propagation. In particular, gravity waves are of interest because their spatial scales are of the same order as infrasonic wavelengths. Gravity waves result from oscillations of air parcels displaced by buoyancy and restored by gravity. The oscillations have time scales ranging from minutes to tens of hours. Vertical length scales of gravity waves are in the range of 0.1 to 15 km, and horizontal scales can span from 10 to 1,000 km. The multi-scale nature of gravity waves presents a challenge to quantification of their properties. Owing to the important influences of gravity waves on the atmosphere's general circulation, vertical structure, and spatiotemporal variability, gravity wave dynamics is a significant atmospheric science research topic area. Recent research progress includes a better understanding of gravity wave source characteristics and evolution with altitude due to changes in wind conditions and atmospheric stability (e.g., Fritts and Alexander, 2003). The development of high-fidelity physically-based gravity wave parameterizations is an active research area.

BBN has previously developed a baseline wind variability model (Norris and Gibson, 2002; Gibson, et al., 2008) for predicting infrasound deviations due to atmospheric effects that are not resolved by the existing atmospheric specifications. The basic variability model uses a power-law wind perturbation spectrum based on the spectral gravity wave model of Gardner (1995, 1993), and generates realizations of horizontal wind perturbation profiles due to gravity waves. A source spectrum is defined near the ground, and as the wave spectrum is propagated up in height, attenuation is modeled by introduction of diffusive damping. Therefore, height-dependent gravity wave dependencies are modeled. Range-dependent effects can be approximated by selecting a dominant horizontal correlation length and combining wind perturbation profiles using Gaussian weighting functions.

Approaches to Improved Gravity Wave Modeling

As discussed above, baseline approaches to modeling infrasound through gravity waves have relied primarily on one-dimensional vertical wavenumber spectral models. This simplified model approach captures the vertical spatial scales in gravity waves as a function of height. We are currently extending this capability by accounting for additional dimensional variability, including horizontal wavenumber.

Furthermore, given a spectral model, numerous parameters must be defined in order to apply it. In the baseline work, a single representative set of parameters was defined for use in all propagation scenarios. In the current effort, spatial and temporal dependencies are considered. For example, parameters may be quantified based on latitude and Julian day. The baseline implementation of the Gardner model does not account for the fact that gravity wave fields can vary dramatically with altitude, latitude, and season (e.g., Eckermann, 1995).

Another shortcoming of the baseline gravity wave model is that it ignores the typically strong refraction of gravity waves by variations in the mean winds and the mean stratification above 15 km. These limitations are being addressed by including the refraction effects of the gravity wave field by the background atmosphere as defined by the G2S specification. There are several existing models that include the effects of refraction on a spectrum of gravity waves (e.g., Fritts and Lu, 1993; Eckermann, 1995; Warner and McIntyre, 2001). These models involve ray-tracing directly in the Fourier domain. They are purely spectral and have not been used to generate a spatial realization of the gravity wave field. For this current application, we have considered a different Fourier formulation that predicts refraction effects locally in the spatial domain and is computationally very fast. The formulation involves ray tracing in Fourier space, in a way that efficiently approximates the vertical eigenfunctions for a given background. The ray solutions are then Fourier synthesized to give the spatial solution. Since wave phases are also computed, a wide range of problems can be considered, from deterministic mountain waves, to semi-deterministic gravity waves generated by convection, to fully random wave fields.

For this application, it is possible to represent a local atmospheric gravity wave field using the summation of vertical eigenfunctions. The associated mathematical expression is

$$w(x,y,z,t) = \sum_{\omega} e^{-i\omega t} \int \int_{-\infty}^{\infty} W(k,l,z) e^{i(kx+ly)} dk dl \qquad (1)$$

where the gravity waves have vertical velocity *w*, frequency *ω*, and horizontal wavenumber components *k*, *l* in the horizontal directions *x*, *y*, respectively. The vertical coordinate is *z* and the time is *t*. A very efficient way to solve for *w* is via ray tracing, and in particular by ray tracing in the Fourier domain (i.e., in *k*, *l* space) with *z* as the parametric variable. In this manner critical layers are handled in a natural way, plus the solution permits no resonant singularities. Trapped waves are represented by a uniform approximation involving the Airy function. Furthermore, if it is assumed that the winds are horizontally homogeneous and stratified over a limited sub-domain then *k* and *l* are constant along each ray. Thus the ray tracing integration is one-dimensional. Another advantage to this approach is that the horizontal variability in the wave field (and the associated horizontal correlation scales) also follows directly from the specified horizontal wavenumber dependence of the wave source spectrum. Self-consistent wave field calculations where the background profiles vary over distances greater than 500 km can also be synthesized via the superposition of several overlapping range independent realizations. Additional theoretical details of the Fourier gravity wave ray tracing method are presented in Broutman et al. (2003, 2006, and 2009). Comparisons with mountain-wave observations are given in Eckermann et al. (2006) and Alexander et al. (2009).

An example of results for the gravity wave field computed from (1) using the Fourier-space ray tracing technique is shown in Figure 1. The left panel shows a random realization of *w* in a uniform background. The right panel shows how the same spectrum of gravity waves is refracted by an idealized wind jet centered at 25 km altitude, with a peak speed of 5 m/s. In this example the gravity wave source height is z = 0. Most of the gravity waves encounter either turning points or critical layers before reaching the center of the wind jet, so the gravity wave field is weak above the wind jet. As expected from linear theory, the largest gravity wave amplitudes occur where the turning points are concentrated, just below the peak of the wind jet. Note that Figure 1 is derived from a two-dimensional calculation. In three dimensions, there is in reality more gravity wave propagation through the wind jet because the refraction weakens as the horizontal propagation direction moves away from the wind direction.

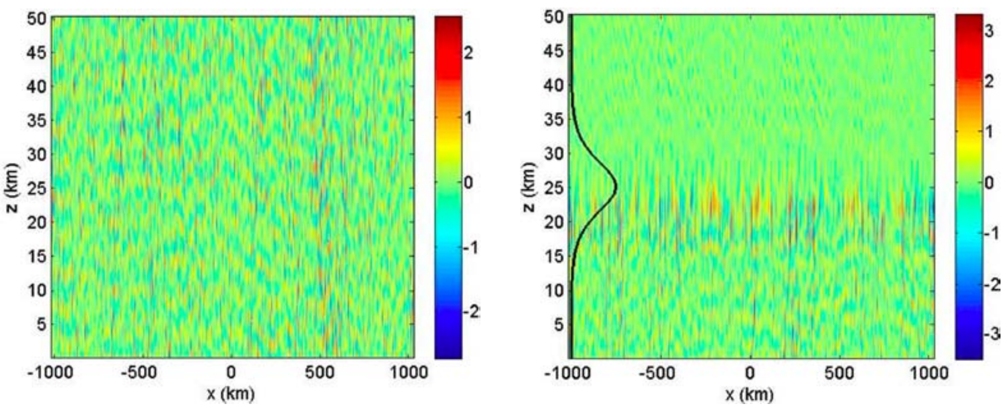

Figure 1. Vertical velocity *w* for a random realization of a spectrum of gravity waves. Left panel: for a uniform background wind; Right panel: for a mean wind jet centered at 25 km altitude, with peak speed 5 m/s (denoted by the bold curve). The solution is calculated with 1024 horizontal wavenumbers on a spatial grid with 2 km grid spacing. Ten frequencies were used for the sum in Eq. (1). The solution has been scaled by exp(-*z*/2*H*), where *H* = 7.5 km is the density scale height.

All of the prerequisites for calculating the vertical and horizontal amplitudes of the random gravity wave perturbations are provided by the available G2S specifications. Stochastic gravity wave perturbation fields (U’, V’, T’, P’ and ρ’), i.e., horizontal wind components, temperature, pressure and density, as a function of z, x, y and t can be calculated given the corresponding G2S background atmospheric fields (U, V, T, P, and ρ) over the same spatial domain z, x, y. This approach accounts for the important seasonal, latitude and longitude dependence of the various auxiliary model parameters, such as the gravity wave spectrum lower cut off wave number (m*), which, together with the background atmospheric state, govern the nature and amplitude of the gravity wave spectrum. Using this methodology, wave perturbation fields are calculated that are self-consistent with the background atmospheric flow.

An example calculation of a self-consistent gravity wave field is presented in the following figures for a regional scenario. Figure 2 shows background atmospheric profiles at two locations separated by 375 km, for an arbitrarily chosen date and time (05:00 UT on 01/11/2002). Altitude-dependent and range-dependent gravity wave perturbations of U, V, W, and T are computed for a 3D data cube (512 km x 512 km x 151 km, with 4 km x 4 km x 1 km resolution). We use a random realization of a realistic gravity wave spectrum (Warner and McIntyre, 2001) launched from an altitude of 15 km. Five frequencies ω are used in this preliminary test case, although the refraction of the gravity waves produces a full range of intrinsic frequencies. Each Fourier component is ray-traced to give an approximation of the vertical eigenfunctions *W*. The ray solutions are then Fourier synthesized via (1) to give the spatial wavefield. Figures 3 and 4 show perturbation fields, over slices of altitude versus range, in an East-West and a North-South plane, respectively. Figure 5 shows the atmospheric profiles including gravity wave perturbations.

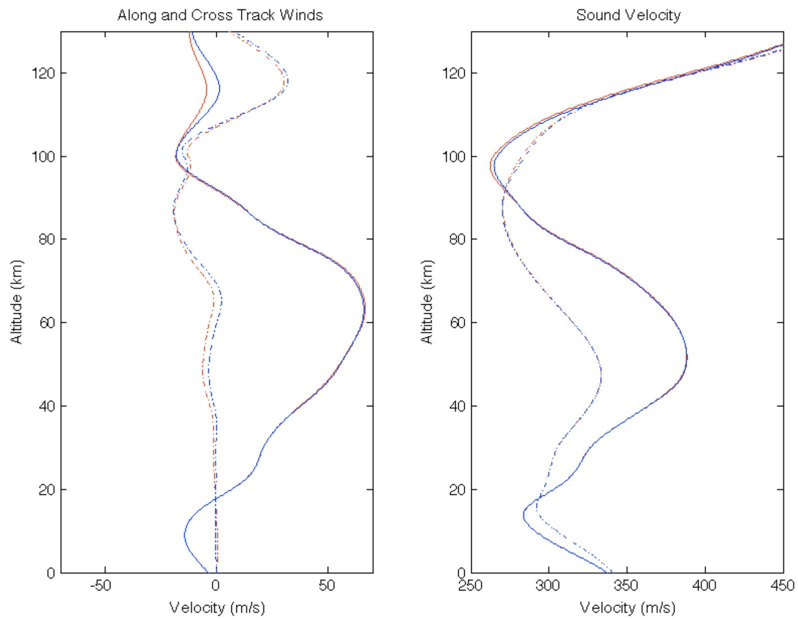

Figure 2. Atmospheric profiles (from HWM-93 and NRLMSISE-00) for a propagation scenario consisting of a source location (red) 375 km east of station I01AR (blue). Along-track winds (+ westward) and effective sound velocities are shown as solid lines. Cross-track (+ northward) winds and effective sound velocities are shown as dashed lines.

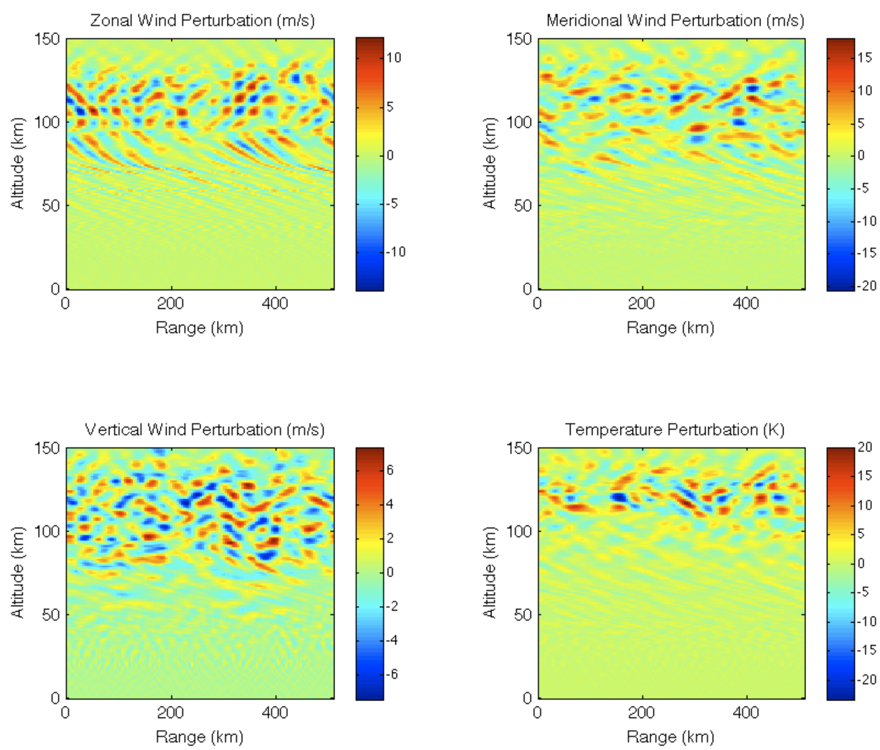

Figure 3. Perturbation fields, altitude vs. range, East-West plane, corresponding to scenario in Figure 2.

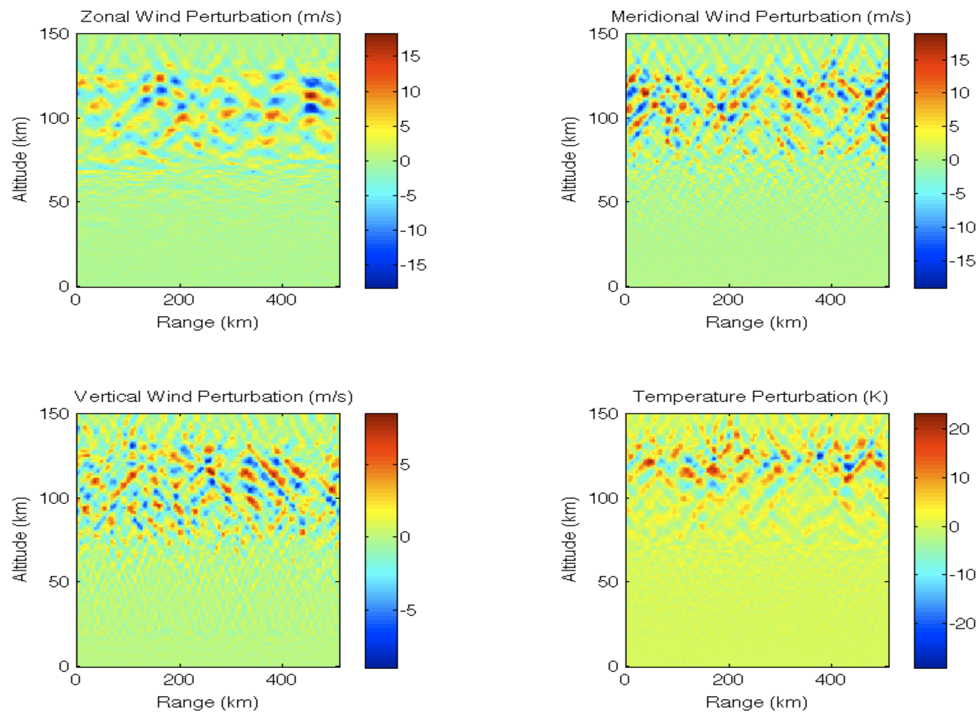

Figure 4. Perturbation fields, altitude vs. range, North-South plane, corresponding to scenario in Figure 2.

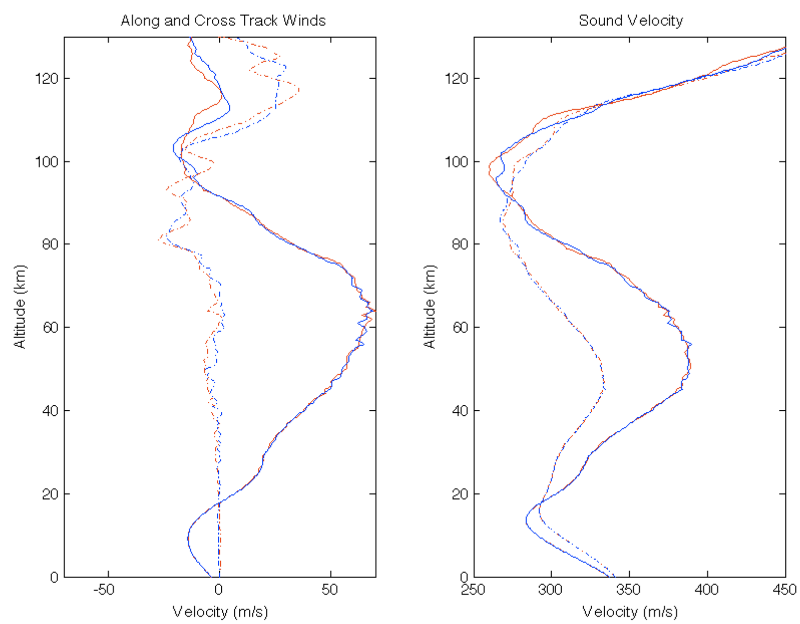

Figure 5. Atmospheric profiles including gravity wave perturbations for the propagation scenario discussed above. Color and line styles are the same as in Figure 2.

It can be observed in the figures that wave amplitudes generally grow with altitude, limited by wave-breaking and ultimately by viscosity above an altitude of about 100 km. In this example, vertical wind perturbations of 7 m/s, temperature perturbations of 20 K, and horizontal wind perturbations of >15 m/s are predicted in the 80 to 130 km altitude region. There is a significant amount of wave-trapping below about 40 km, most clearly indicated by the more vertically oriented wave phases in the vertical velocity plots (lower left panels of Figures 3 and 4). The trapped waves have shorter horizontal scales, leaving longer scales at higher altitudes.

Applications to Infrasound Propagation Modeling for Ground-Truth Events

The G2S atmospheric specifications described above, the baseline gravity wave models due to Gardner, and a suite of infrasound propagation models (including 3D ray-tracing, parabolic equation (PE), time-domain parabolic equation (TDPE), and normal modes) are currently integrated into the tool kit InfraMAP (Gibson and Norris, 2002; Norris and Gibson, 2004). InfraMAP (*Infrasonic Modeling of Atmospheric Propagation*) has been developed by BBN for use in the study of infrasound propagation and monitoring. InfraMAP can be applied to predict attenuation, travel times, bearings, amplitudes, and waveforms for infrasonic events. The most recent version of InfraMAP includes TDPE waveform prediction capabilities (Tappert et al., 1995) based on either a canonical blast wave or any user-defined source waveform. PE and TDPE calculations incorporate effects of horizontal wind components (both mean and perturbations) by utilizing the effective sound speed approximation.

Using the baseline gravity wave model, propagation studies have been conducted for various scenarios and ground truth events. An example to quantify gravity wave effects on infrasound propagation is the Ghislenghien, Belgium, gas pipe explosion of 30 July 2004. (Evers and Haak, 2006) This event was a surface explosion of approximately 40 tons yield. It was detected at arrays throughout Europe. Here we consider the 379 km path to the Flers, France, infrasound station. Figure 6 shows the PE amplitude field predictions at 1.0 Hz for the cases in which fine-scale gravity wave perturbations are excluded and included. The mean atmospheric profiles were defined using range-dependent G2S specifications. The propagation modeling includes effects of atmospheric absorption in the thermosphere (Sutherland and Bass, 2004), which can be seen to strongly reduce predicted amplitudes of thermospheric arrivals. Stratospheric ducting can be observed in the model predictions. Without gravity wave perturbations, little energy penetrates the stratospheric shadow zone and reaches the receiver location. With gravity wave perturbations, additional scattered energy is predicted to penetrate the shadow zone and reach the receiver.

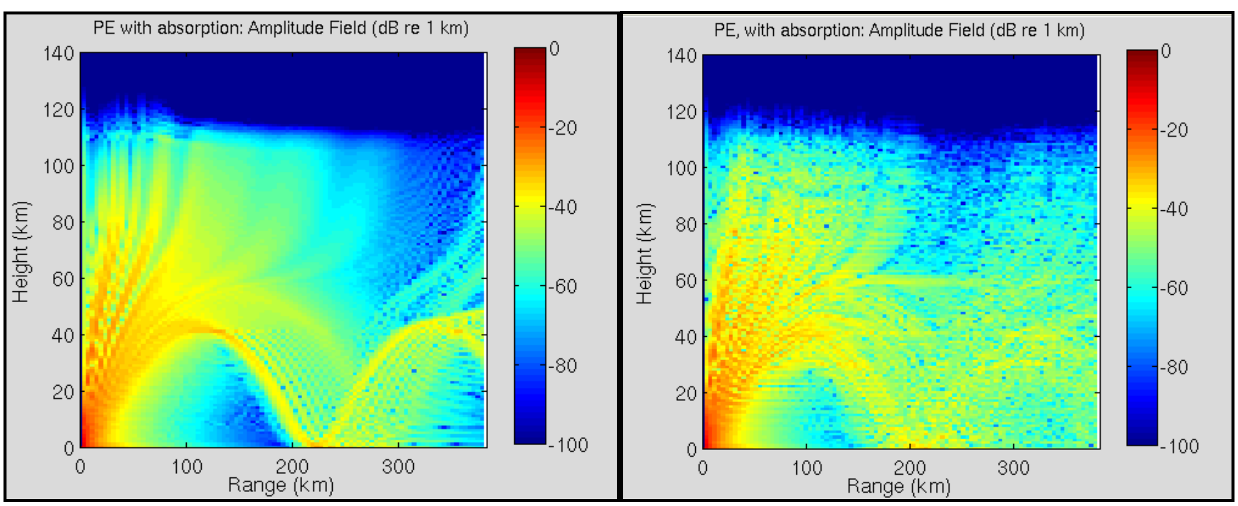

Figure 6. PE amplitude predictions at 1.0 Hz without gravity waves (left panel) and with gravity waves (right panel), for infrasound propagation from the Ghislenghien, Belgium, explosion to Flers, France.

A TDPE waveform prediction along the same propagation path is shown in Figure 7. The TDPE simulation presented here is computed over a bandwidth of 0-4 Hz and includes effects of gravity wave perturbation. With gravity waves, waveform predictions show substantial received energy. Three phases are predicted in the synthetic waveform and the arrival times of these three phases are consistent with those in the observation at Flers as reported by Evers and Haak (2006).

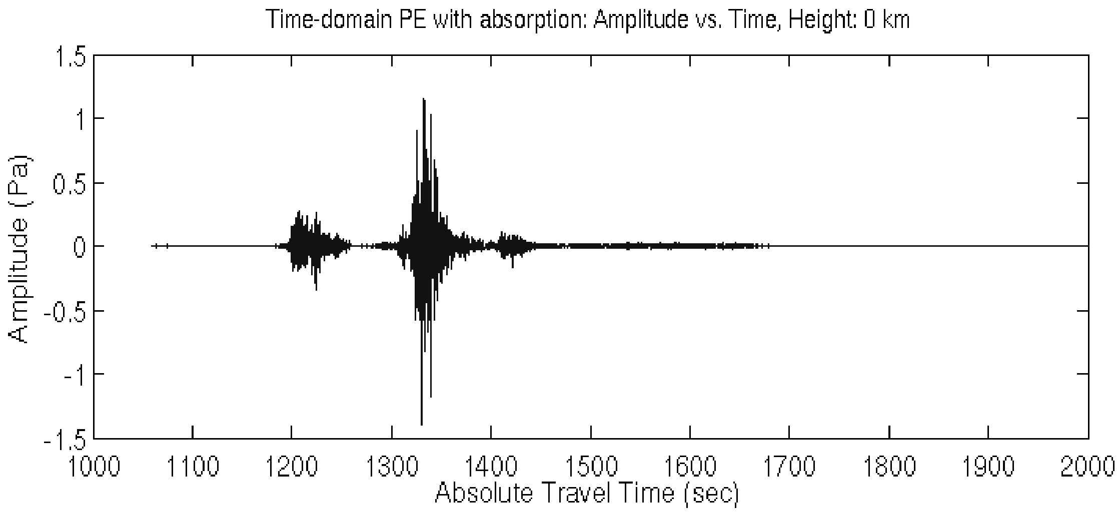

Figure 7. TDPE synthetic waveform, computed over 0 - 4.0 Hz bandwidth, including gravity wave perturbation, for infrasound propagation from the Ghislenghien, Belgium, explosion to Flers, France.

An additional example is presented for the Buncefield, England, fuel tank explosion of 11-Dec-2005. (Ceranna et al., 2007) This event was a surface explosion of approximately 30 tons yield. It was detected at arrays throughout Europe. Here we consider the 334 km path to the Flers, France, infrasound station. Figure 8 shows the TDPE simulation computed over a bandwidth of 0-4 Hz, including the effects of gravity wave perturbation.

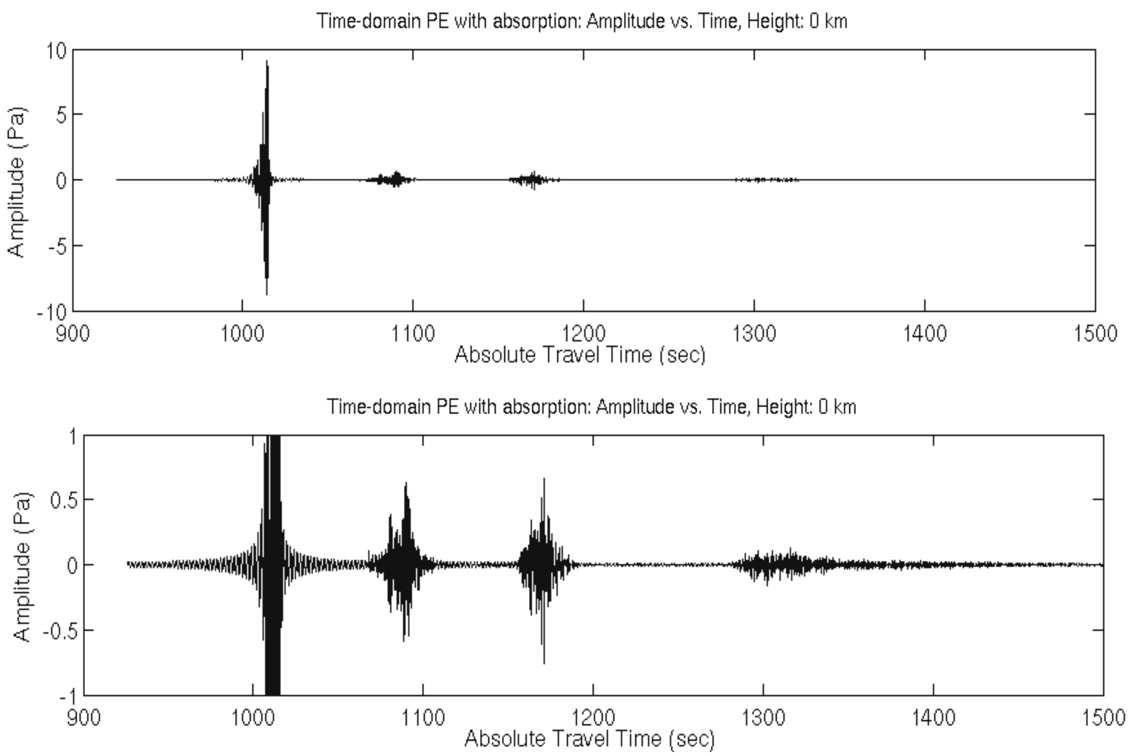

Figure 7. TDPE synthetic waveform, computed over 0 - 4.0 Hz bandwidth, including gravity wave perturbation, for infrasound propagation from the Buncefield, England, explosion to Flers, France. The synthetic waveform is shown using two different amplitude scales in the upper and lower panels.

The mean atmospheric profiles were defined using range-dependent G2S specifications, and effects of thermospheric absorption are included. Four phases are predicted in the synthetic waveform and the arrival times of these four phases are consistent with those in the observation at Flers as reported by Ceranna et al. (2007).

CONCLUSIONS AND RECOMMENDATIONS

Substantial evidence for the importance of atmospheric variability due to fine-scale inhomogeneity has been indicated by TDPE waveform predictions for events observed at regional ranges. In several instances, conventional propagation modeling has failed to predict observed arrivals due to the lack of a stratospheric duct in the baseline atmospheric characterization; these observations exist in so-called “shadow zones.” However, modeled infrasound arrivals that consider energy refracted or scattered from gravity waves agree well in waveform shape, extent and arrival time with observations. These results indicate the considerable benefit to regional monitoring that is to be gained by understanding gravity wave effects on infrasound. While implementation of our existing baseline gravity wave model enables prediction of certain infrasound features, there is significant additional understanding of the fundamental physics yet to be gained and additional model fidelity that is needed.

We will continue extension of the new gravity wave calculation technique to the full 3D domain, integrating calculations with G2S mean atmospheric profiles for scenarios of interest, and considering horizontally varying mean fields of wind and density. We will also explore the numerical parameter space for source spectrum shape constants, empirical wave amplitude normalization scale factors, wave-breaking, viscosity characterization, and the optimal source spectrum seeding altitude. The formulation allows a range of frequencies ω in (1), but work so far has concentrated on source spectra with one or a few frequencies, for computational simplicity. We will investigate optimal frequency discretizations for source spectra, using a fuller range of frequencies. The new gravity wave perturbation fields will be incorporated with existing infrasound propagation models. The new formulations will be tested, compared against baseline models, and used to study additional infrasound ground truth events of interest.

REFERENCES

Alexander, M. J., S. D. Eckermann, D. Broutman, and J. Ma (2009). Momentum flux estimates for South Georgia Island mountain waves in the stratosphere observed via satellite, *Geophys. Res. Lett.*, 36, L12816, doi:10.1029/2009GL038587.

Bhattacharyya, J., H. Bass, D. Drob, R. Whitaker, D. ReVelle, and T. Sandoval (2003). Description and Analysis of Infrasound and Seismic Signals Recorded from the Watusi Explosive Experiment, in *Proceedings of the 25th Seismic Research Review—Nuclear Explosion Monitoring: Building the Knowledge Base,* LA-UR-03-6029, Vol. 2, pp. 587–596.

Broutman, D., J. W. Rottman, and S. D. Eckermann (2003). A simplified Fourier method for nonhydrostatic mountain waves. *J. Atmos. Sci*., 60, 2686-2696.

Broutman, D., J. Ma, S.D. Eckermann, and J. Lindeman (2006). Fourier-ray modeling of transient trapped lee waves. *Mon. Wea. Rev*., 134, 2849-2856.

Broutman, D., S. D. Eckermann, and J. W. Rottman (2009). Practical application of two turning-point theory to mountain-wave transmission through a wind jet, *J. Atmos. Sci*., 66, 481-494.

Ceranna, L., D. Green, A. Le Pichon and P. Mialle (2007). The Buncefield Explosion: A benchmark for infrasound analysis in Europe, *Proceedings of the Infrasound Technology Workshop*, Tokyo.

Drob, D. P., J.M. Picone, and M.A. Garcés (2003). The Global Morphology of Infrasound Propagation, *J. Geophys. Res.* 108: doi:10.1029/2002JD003307.

Drob, D. P. (2004). Atmospheric Specifications for Infrasound Calculations, *Inframatics*, No. 5.

Drob, D.P., *et al*. (2008). An empirical model of the Earth’s horizontal wind fields: HWM07, *J. Geophys. Res.*, 113, A12304, doi:10.1029/2008JA013668.

Eckermann, S. D. (1995). Effect of background winds on vertical wavenumber spectra of atmospheric gravity waves, *J. Geophys. Res.* 100: 14,097–14,112.

Eckermann, S.D., D. Broutman, J. Ma and J. Lindeman (2006). Fourier-ray modeling of short wavelength trapped lee waves observed in satellite imagery near Jan Mayen. *Mon. Wea. Rev*., 134, 2830-2848.

Evers, L. and H. Haak (2006). Seismo-acoustic analysis of explosions and evidence for infrasonic forerunners, *Proceedings of the Infrasound Technology Workshop*, Fairbanks.

Fritts, D. C., and W. Lu (1993). Spectral estimates of gravity wave energy and momentum fluxes, II: Parameterization of wave forcing and variability, *J. Atmos. Sci.* 50: 3695–3713.

Fritts, D. C., and J. M. Alexander (2003). Gravity Wave Dynamics and Effects in the Middle Atmosphere, *Rev. of Geophys.* 41: 1, 1003.

Gardner, C. (1993). Gravity Wave Models for the Horizontal Wave Number Spectra of Atmospheric Velocity and Density Fluctuations, *JGR* 98; D1, 1035–1049.

Gardner, C. (1995). Scale-Independent Diffusive Filtering Theory of Gravity Wave Spectra in the Atmosphere, *The Upper Mesosphere and Lower Thermosphere: A Review of Experiment and Theory*, Geophysical Monograph 87, AGU.

Gibson, R., and D. Norris (2002). Development of an Infrasound Propagation Modeling Tool Kit, *Defense Threat Reduction Agency Technical Report DTRA-TR-99-47*, Alexandria, VA.

Gibson, R. G., D. E. Norris and D. P. Drob (2008). Investigation of the effects of fine-scale atmospheric inhomogeneities on infrasound propagation, in *Proceedings of the 30th Seismic Research Review—Ground-Based Nuclear Explosion Monitoring Technologies*, LA-UR-08-05261, Vol. 2, pp. 872–881.

Hedin, A.E., E.L. Fleming, A.H. Manson, F.J. Scmidlin, S.K. Avery, R.R. Clark, S.J. Franke, G.J. Fraser, T. Tsunda, F. Vial, and R.A. Vincent (1996). Empirical Wind Model for the Upper, Middle, and Lower Atmosphere, *J. Atmos. Terr. Phys.* 58: 1421–1447.

Kulichkov, S.N. (2004). Long-range propagation and scattering of low-frequency sound pulses in the middle atmosphere, *Met. Atmos. Phys*. 85: No. 1–3, pp. 47–60.

Mutschlecner, J., and R. Whitaker (2006). *Infrasonic Signals from the Henderson, Nevada, Chemical Explosion*, LA-UR-06-6458.

Norris, D., and R. Gibson (2002). InfraMAP Enhancements: Environmental/Propagation Variability and Localization Accuracy of Infrasonic Networks, in *Proceedings of the 24th Seismic Research Review—Nuclear Explosion Monitoring: Innovation and Integration*, LA-UR-02-5048, Vol. 2, pp. 809–813.

Norris, D., and R. Gibson (2004). Advanced Tools for Infrasonic Modeling, *Inframatics*, No. 5.

Picone, J., A. Hedin, D. Drob, and A. Aiken (2002). NRLMSISE-00 empirical model of the atmosphere: statistical comparisons and scientific issues, *J. Geophys. Res.* 107: 1468.

Sutherland, L. and H. Bass (2004). Atmospheric absorption in the atmosphere up to 160 km. *J. Acoust. Soc. Am.*, 115, 1012-1032.

Tappert, F., J.L. Spiesberger, and L. Boden (1995). New full-wave approximation for ocean acoustic travel time predictions, *J. Acoust. Soc. Am*., 97, 2771-2782.

Warner, C.D., and M.E. McIntyre (2001). An ultrasimple spectral parameterization for nonorographic gravity waves, *J. Atmos. Sci.* 58: (14), 1837–1857.